Acta Crystallographica Section F
Structural Biology and Crystallization Communications
ISSN 1744-3091

A C-terminal segment of the V_1R vasopressin receptor is unstructured in the crystal structure of its chimera with the maltose-binding protein

Nallini Vijayarangan Adikesavan,[a]‡ Syed Saad Mahmood,[a]‡ Nithianantham Stanley,[a]‡ Zhen Xu,[a] Nan Wu,[a] Marc Thibonnier[b] and Menachem Shoham[a]*

[a]Department of Biochemistry, School of Medicine, Case Western Reserve University, 10900 Euclid Avenue, Cleveland, OH 44106-4935, USA, and [b]Department of Medicine, School of Medicine, Case Western Reserve University, 10900 Euclid Avenue, Cleveland, OH 44106-4935, USA

‡ These authors contributed equally.

Correspondence e-mail: mxs10@case.edu

Received 31 August 2004
Accepted 7 March 2005
Online 24 March 2005

PDB Reference: MBP-V_1(Ct), 1ytv, r1ytvsf.

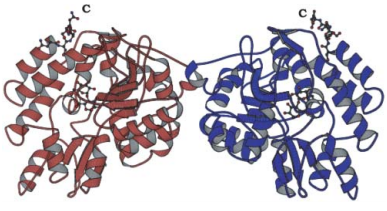

The V_1 vascular vasopressin receptor (V_1R) is a G-protein-coupled receptor (GPCR) involved in the regulation of body-fluid osmolality, blood volume and blood pressure. Signal transduction is mediated by the third intracellular loop of this seven-transmembrane protein as well as by the C-terminal cytoplasmic segment. A chimera of the maltose-binding protein (MBP) and the C-terminal segment of V_1R has been cloned, expressed, purified and crystallized. The crystals belong to space group $P2_1$, with unit-cell parameters $a = 51.10$, $b = 66.56$, $c = 115.72$ Å, $\beta = 95.99^\circ$. The 1.8 Å crystal structure reveals the conformation of MBP and part of the linker region of this chimera, with the C-terminal segment being unstructured. This may reflect a conformational plasticity in the C-terminal segment that may be necessary for proper function of V_1R.

1. Introduction

The antidiuretic hormone arginine vasopressin is a cyclic peptide that regulates free-water reabsorption, body-fluid osmolality, blood volume, blood pressure and cell proliferation *via* activation of specific G-protein-coupled receptors (GPCRs) classified into three distinct receptor subtypes: V_1-vascular (V_1R), V_2-renal (V_2R) and V_3-pituitary (V_3R) (Thibonnier *et al.*, 1998; Thibonnier, Plesnicher *et al.*, 2001). Signal transduction across these seven-transmembrane receptors is mainly mediated by the third intracellular loop (il3) as well as the C-terminal segment (Ct). The C-terminus of the human V_1R is instrumental in receptor trafficking and facilitates the interaction between the intracellular loops of the receptor, the G proteins and coupling to phospholipase C (Thibonnier, Coles *et al.*, 2001). Furthermore, we have shown that agonist stimulation of vasopressin receptors leads to receptor subtype-specific interactions with G-protein-coupled receptor kinases and protein kinase C through specific motifs present in the C-termini of the receptors (Berrada *et al.*, 2000). Direct evidence for the involvement of il3 as well as the cytoplasmic C-terminus in signal transduction has recently been obtained (Nan Wu, unpublished results).

There is very little direct structural information available on GPCRs. Rhodopsin is the only GPCR with a known three-dimensional structure (Palczewski *et al.*, 2000), but even in the crystal structure of rhodopsin the loops are not very well defined. Moreover, there is great variability in the length and in the sequence of the loops as well as the N-terminal and C-terminal segments.

Whereas the C-terminal segment of rhodopsin is 40 residues long, the corresponding region in V_1R is about 57 residues long.

The maltose-binding protein (MBP) is a stable and highly soluble protein from the periplasm of *Escherichia coli*. It has been widely used as a fusion tag to aid in the preparation of recombinant proteins. Recently, it has also been used as a crystallization tag (Smyth *et al.*, 2003). Once crystals of the fusion protein have been formed and X-ray data have been collected, the MBP crystal structure can serve as a molecular-replacement search model.

In order to gain structural information about the C-terminal cytoplasmic segment of V_1R, we have undertaken crystallographic studies of its fusion protein with MBP [MBP-V_1R(Ct)]. Here, we

report the structure of this fusion protein at a resolution of 1.8 Å. Unfortunately, the electron density does not extend beyond the linker region and the C-terminal part of the V_1R is unstructured in this crystal form. This account may thus serve as a cautionary example of an engineered hybrid protein in which the segment of hitherto unknown structure is disordered in the crystal structure. It may, however, be a reflection of an increasing awareness that some proteins need to be unstructured in order to function properly (Wright & Dyson, 1999).

2. Protein expression and purification

The human V_1R C-terminal DNA sequence was amplified from the human V_1R cDNA clone using the oligonucleotides V_1A-CTERM-SENSE (5′-GCTGCTGGATCCAGCTTCCCATGCTGCCAAAAC-3′) and CTERM-PSV282-ANTI (5′-ACTACTCTCTCGAGTCAT-CAAGTTGAAACAGGAATGAATTT-3′). The DNA segment was digested with *Bam*HI and *Xho*I restriction enzymes and ligated into a modified plasmid pSV282 (kindly provided to us by Laura Mizoue at Vanderbilt University) incorporating the His_6-MBPV_1R C-terminal tail (Fig. 1). The construct was verified by DNA sequencing. The construct expressed the residues 362–418 of V_1R as an MBP-fusion protein. As seen in Fig. 2, this segment comprises the intracellular C-terminus of V_1R.

A 4.8 l volume of Luria–Bertani (LB) broth was inoculated with an overnight 100 ml culture. The culture contained *E. coli* strain BL21 (Novagen) harboring the modified pSV282 plasmid supplemented with kanamycin (100 µg ml^{-1}). Expression of the fusion protein was induced with 0.1 m*M* isopropyl-*β*-D-thiogalactopyranoside (IPTG) at OD_{600} = 0.6. This growth phase was extended for 3 h and the cells were spun for 30 min at 6000 rev min^{-1}. The cells were stored overnight at 253 K, thawed and agitated. Cell lysis was performed by sonication (Branson Digital Sonifier). The lysis buffer consisted of 50 m*M* PBS ($Na_2HPO_4{\cdot}7H_2O$ + $NaH_2PO_4{\cdot}H_2O$) pH 7.4, 300 m*M* NaCl and 0.1 m*M* phenylmethanesulfonyl fluoride (PMSF). The broken cells were spun at 10 000 rev min^{-1} for half an hour. The supernatant was mixed with cobalt affinity resin (BD Biosciences) and poured into the column. The column was washed with the same lysis buffer without and with addition of 5 m*M* imidazole. The protein was eluted with a 200 ml imidazole gradient (5–500 m*M*). SDS–PAGE revealed the presence of three bands in the eluted fractions.

```
1                15                                                    75
MGSSHHHHHHGSSMKIEEGKLVIWINGDKGYNGLAEVGKKFEKDTGIKVTVEHPDKLEEKFPQVAATGDGPDIIF
                                                                      150
WAHDRFGGYAQSGLLAEITPDKAFQDKLYPFTWDAVRYNGKLIAYPIAVEALSLIYNKDLLPNPPKTWEEIPALD
                                                                      225
KELKAKGKSALMFNLQEPYFTWPLIAADGGYAFKYENGKYDIKDVGVDNAGAKAGLTFLVDLIKNKHMNADTDYS
                                                                      300
IAEAAFNKGETAMTINGPWAWSNIDTSKVNYGVTVLPTFKGQPSKPFVGVLSAGINAASPNKELAKEFLENYLLT
                                                                      375
DEGLEAVNKDKPLGAVALKSYEEELAKDPRIAATMENAQKGEIMPNIPQMSAFWYAVRTAVINAASGRQTVDEAL
          386                 362
KDAQTNSSSNNNNNNNNNNLGIEENLYFQGSSFPCCQNMKEKFNKEDTDSMSRRQTFYSNNRSPTNSTGMWKDSP
            418
KSSKSIKFIPVST
```

Figure 1
Amino-acid sequence of the His_6-MBP-V_1R(Ct) fusion protein in single-letter code. The color scheme is as follows: orange, His_6 tag; blue, MBP; red, linker with tobacco etch virus (TEV) protease cleavage sequence ENLYFQGS; black, C-terminal segment of V_1R. Residue numbers in bold are according to the V_1R numbering scheme as shown in Fig. 2.

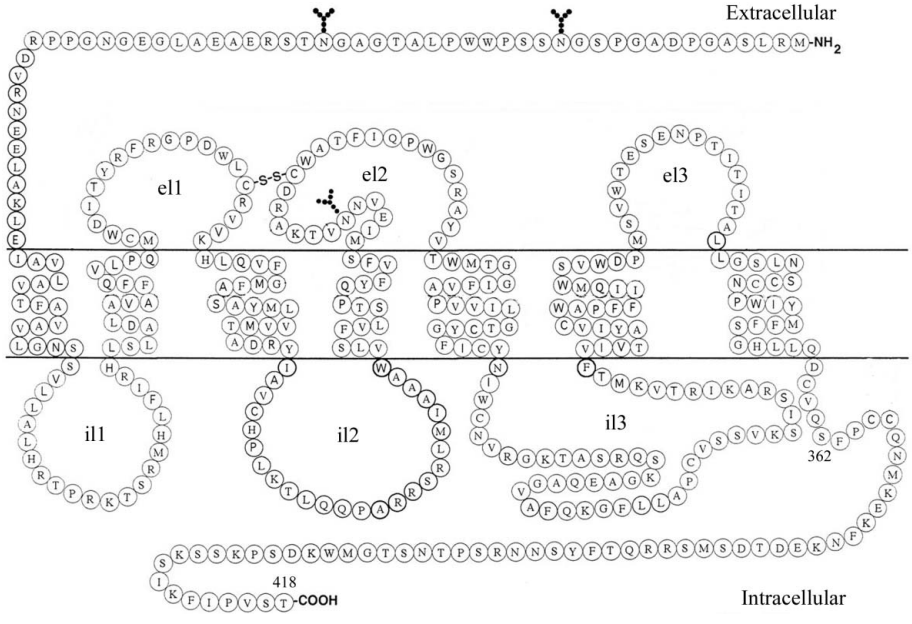

Figure 2
Schematic diagram of the human V_1 vascular vasopressin receptor. Amino-acid residues are depicted in single-letter code. Carbohydrate-attachment sites are shown by black circles forming the letter Y. Extracellular and intracellular loops are delineated el1, el2, el3, il1, il2 and il3, respectively. Residue numbers indicate the boundaries for the C-terminal segment used to engineer the chimera with MBP.

Table 1
X- ray data-collection and refinement statistics.

Values in parentheses refer to the highest resolution shell.

Data collection	
Space group	$P2_1$
Unit-cell parameters (Å, °)	a = 51.10, b = 66.56, c = 115.72, β = 95.99
No. of molecules per AU	2
V_M (Å^3 Da^{-1})	2.0
Solvent content†	0.39
Resolution (Å)	1.80
Unit-cell volume (Å^3)	391446
R_{merge}	0.076 (0.43)
Completeness	99.2
$\langle I/\sigma(I)\rangle$	16.8 (2.8)
Wavelength used (Å)	0.97934
Mosaicity (°)	0.43
Total No. of reflections	238700
No. of unique reflections	71440
Redundancy	3.7
Refinement	
Resolution range (Å)	34.43–1.80
Reflections	71204
R_{cryst}	0.200
R_{free}‡	0.224

† Based on a molecular weight of 50 kDa. ‡ 5% of the data were used for cross-validation.

Further purification was performed on an amylose affinity column (New England Biolabs) to which the MBP moiety binds. The protein was eluted with 10 m*M* maltose in 50 m*M* Na_2HPO_4, 0.15 *M* NaCl, 0.1 m*M* PMSF pH 7.5. The purified protein migrates as a single band on SDS–PAGE with an approximate molecular weight of 50 kDa (Fig. 3*a*).

3. Crystallization

The protein was dialyzed four times against a solution containing 10 m*M* HEPES buffer pH 7, 100 m*M* NaCl and 0.02% NaN_3 and was concentrated to 14.5 mg ml^{-1} using a Centricon concentrator (Amicon Corporation) with a 5 kDa cutoff filter. Crystallization experiments were set up in hanging drops using vapor diffusion with Hampton Crystal Screens I and II (Hampton Research, Riverside, CA, USA). Drops were prepared by mixing 1 µl protein solution with 1 µl reservoir solution.

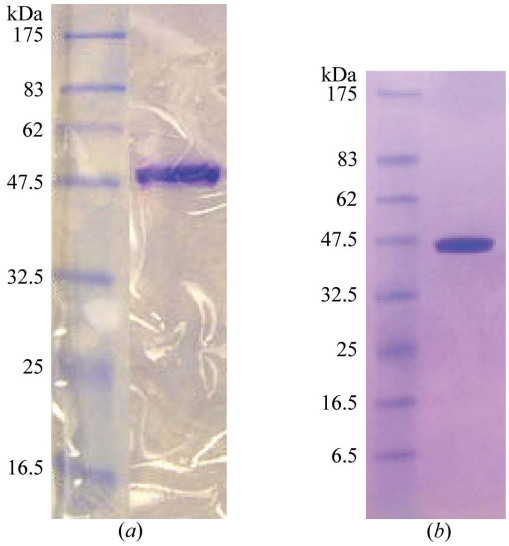

Figure 3
(*a*) SDS–PAGE of the purified His_6-MBP-V_1R(Ct) fusion protein. (*b*) SDS–PAGE of dissolved crystals.

4. Data collection, structure solution and structure refinement

X-ray data were collected at synchrotron beamline BM19 of the Structural Biology Center at the Advanced Photon Source (APS), Argonne National Laboratory, Illinois, USA. All diffraction images were processed using *DENZO* and the integrated intensities were scaled and analyzed using *SCALEPACK* from the *HKL*2000 package (Otwinowski & Minor, 1997). Crystallographic data are shown in Table 1. The structure was solved by molecular replacement using the program *CNS* (Brünger *et al.*, 1998). The coordinates of the MalE-B363 structure (PDB code 1a7l; Saul *et al.*, 1998) were used as the search model. The rotation search, carried out with the fast direct rotation function in the resolution range 15–4 Å, revealed two outstanding solutions. A subsequent translation search at the same resolution range resulted in clear-cut solutions for the two molecules in the asymmetric unit. Upon rigid-body refinement to 1.8 Å, the values for R_{cryst} and R_{free} were both 0.39. The molecular-replacement model was refined by simulated annealing with *CNS* (Brünger *et al.*, 1998). Model building was carried out in *O* (Jones *et al.*, 1991) using $2F_o - F_c$ and $F_o - F_c$ electron-density maps.

5. Results and discussion

The structure of MBP-V_1R(Ct) was refined to a resolution of 1.8 Å with good refinement statistics. The final R_{cryst} and R_{free} are 0.200 and 0.224, respectively. 92% of the residues are in most favored regions of the Ramachandran plot, with the remainder in allowed regions, as analyzed with *PROCHECK* (Laskowski *et al.*, 1993). The fusion protein His_6-MBPV_1R(Ct) encompasses the sequence of MBP, a 26-residue linker and a 57-residue C-terminal segment of V_1R (Figs. 1 and 2). This fusion protein was purified to homogeneity (Fig. 3). Single crystals were obtained from 0.2 *M* ammonium sulfate, 30%(*w*/*v*) PEG 8000 at 295 K. The prismatic crystals grew to dimensions of 0.3 × 0.2 × 0.1 mm within 15 d (Fig. 4). For cryo-protection, crystals were submerged for a few seconds in a solution consisting of 0.2 *M* ammonium sulfate, 25%(*v*/*v*) PEG 400 and 25%(*v*/*v*) glycerol. The crystals were flash-frozen in a stream of gaseous nitrogen at 100 K and stored in liquid nitrogen for X-ray diffraction experiments.

5.1. Overall structure

The model includes residues 15–386 in chain *A* and 15–385 in chain *B*, one maltose moiety for each molecule and 640 water molecules

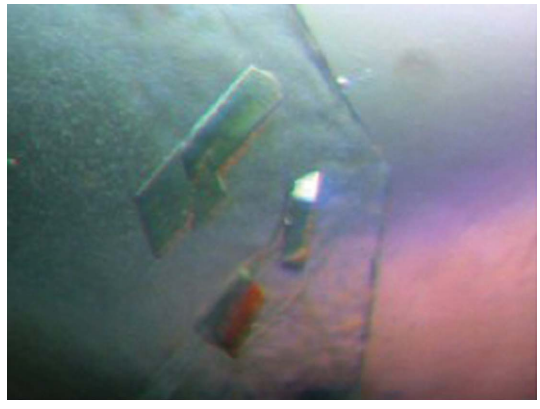

Figure 4
Crystals of the His_6-MBP-V_1R(Ct) fusion protein. These crystals grow to dimensions of 0.3 × 0.2 × 0.1 mm.

(Fig. 5). The structure reflects the closed conformation of the maltose-binding protein. The 14 residues of the hexahistidine tag at the N-terminus as well the first residue of MBP are disordered in both molecules of the asymmetric unit. Likewise, the C-terminal segment of V_1R is unstructured in both molecules, although there would be ample space in the crystals for the 83 residues of the linker and the C-terminal segment. Only the first six and five residues of the linker region following the MBP structure are ordered in molecules *A* and *B*, respectively (Fig. 6). It is likely that the protein in the crystals may have degraded somewhat, since the protein from dissolved crystals migrates a little faster than the purified protein prior to crystallization (Fig. 3). However, it seems that the bulk of the chimera is still present in the crystals, since the apparent molecular weight is significantly higher than 40 kDa, the molecular weight of MBP alone.

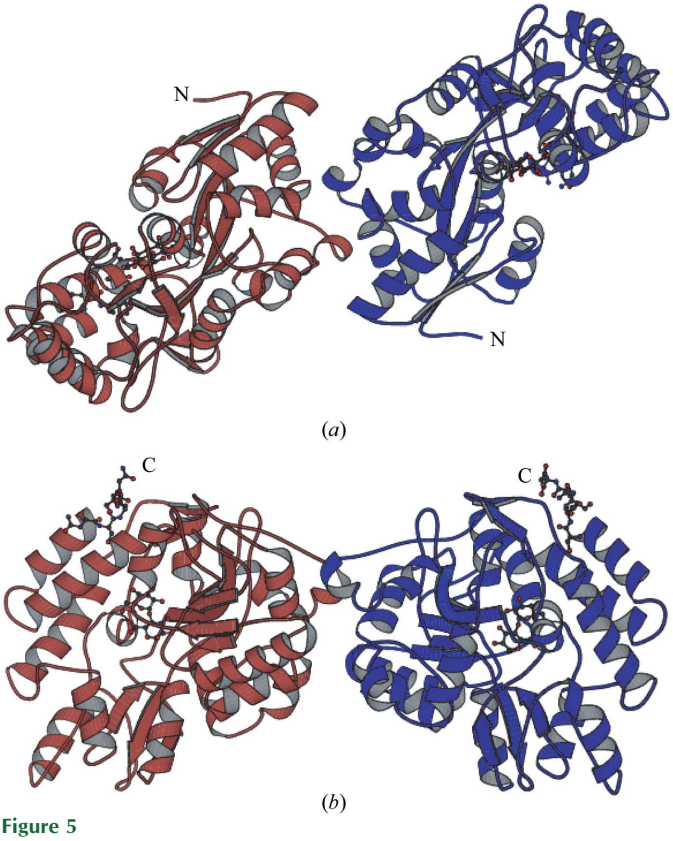

Figure 5
Ribbon diagrams of the two molecules in the asymmetric unit of the crystals. Maltose moieties and the linker region are shown in ball-and-stick conformation. The termini are labeled N and C, respectively. (*a*) View down the non-crystallographic dyad; (*b*) view along the non-crystallographic dyad.

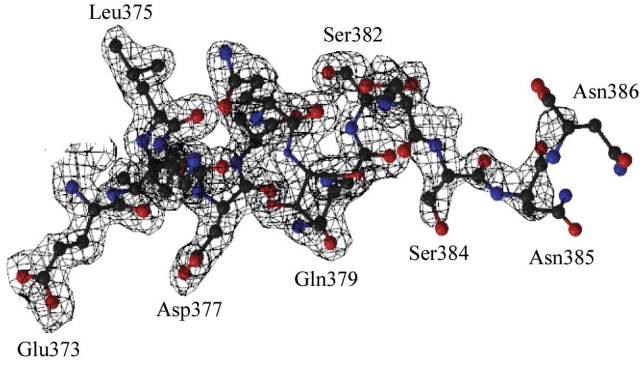

Figure 6
The C-terminal portion of the model visible in a $2F_o - F_c$ electron-density map contoured at one standard deviation above the mean density. Residues 373–386 of molecule *A* are shown in ball-and stick representation. There is no electron density beyond Asn386, which is the sixth residue of the linker between the maltose-binding protein and the C-terminal segment of the V_1R vasopressin receptor. For molecule *B* there is no density beyond Asn385 (data not shown).

The unstructured nature of the C-terminal segment may reflect its conformation within the structure of the intact V_1R receptor. Having an unstructured intracellular C-terminal segment may be important for the proper function of the receptor. However, this segment must become at least partially ordered upon interaction with arrestin-2 and other protein-binding partners (Nan Wu, unpublished results). Conformational plasticity may be a requirement for proper signaling and phosphorylation may also play a role in this process.

5.2. The molecular interface and packing interactions

The two molecules of MBP-V_1(Ct) in the asymmetric unit are related by a non-crystallographic dyad (Fig. 5). The two molecules are virtually identical, with an r.m.s. deviation of 0.38 Å between corresponding C^{α} positions. It is somewhat surprising and interesting to note that the twofold symmetrical molecular interface is predominantly formed by hydrogen bonds between acidic residues mediated by intervening water molecules (Fig. 7). Crystal structures of MBP-fusion proteins have been reported with one, two or three molecules per asymmetric unit (Smyth *et al.*, 2003). MBP fusion proteins with SarR (Liu *et al.*, 2001) and ribosomal protein L30 (Chao *et al.*, 2003) have been crystallized with two molecules per asymmetric unit. The interface between the two molecules of MBP-SarR in the asymmetric unit is formed by extensive hydrophobic contacts between the SarR domains, whereas in the MBP-L30 structure the molecular interface is formed by contacts between the two MBP moieties in the asymmetric unit. In MBP-V_1(Ct) the contacts are also between MBP moieties but the interface is completely different compared with that in MBP-L30 or in MBP-maltose (Fig. 8).

The MalE-B363 structure (PDB code 1a7l; Saul *et al.*, 1998) was used as a molecular-replacement search model since it comprises an MBP-fusion protein with a peptide. However, the packing is very different from the MBP-V_1(Ct) crystal structure. The MalE-B363 protein crystallizes with three molecules per asymmetric unit, whereas MBP-V_1(Ct) has two molecules in the asymmetric unit. The

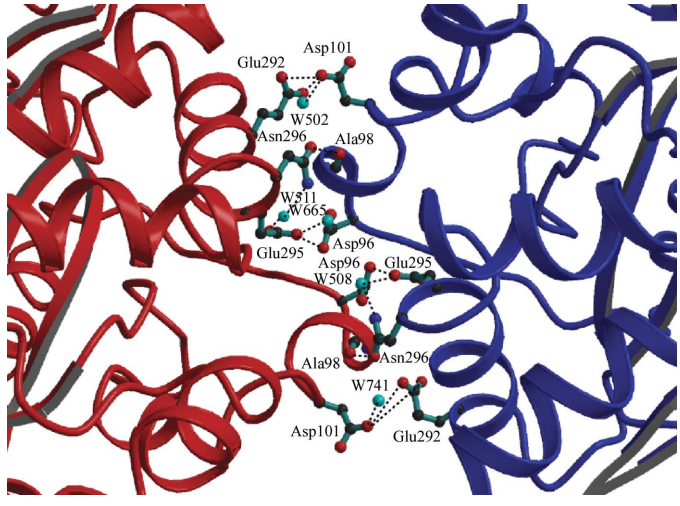

Figure 7
The dimer interface between the two MBP molecules related by a local twofold axis is predominantly formed by hydrogen bonds between acidic residues mediated by intervening water molecules. The two MBP molecules are shown as red and blue ribbon. Residues involved in intersubunit contacts are depicted in ball-and-stick representation. Water molecules are shown as cyan spheres labeled W. Hydrogen bonds are shown as dashed lines.

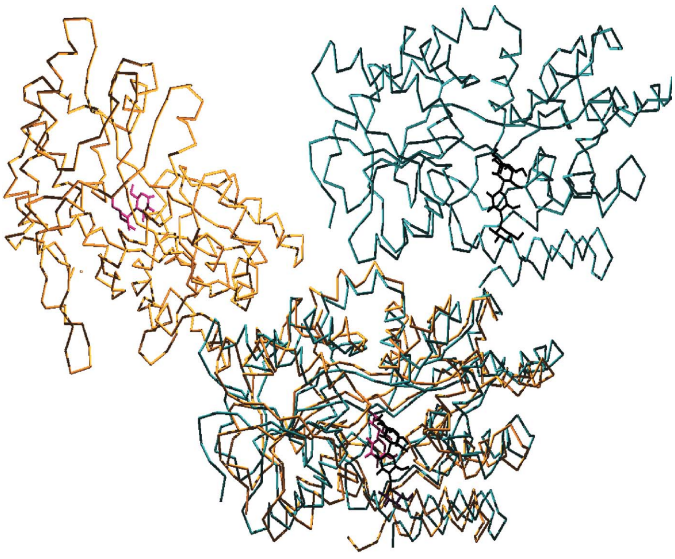

Figure 8
Intermolecular packing of MBP in the dimeric crystal structures of MBP-V_1(Ct) and a maltose–MBP complex (Duan & Quiocho, 2002; PDB code 1ez9). C^{α} diagrams of MBP-V_1(Ct) and maltose–MBP are shown in green and blue, respectively. Maltose moieties are shown in stick representation. The superposition of chain *A* in both crystal structures is shown at the bottom center. The surfaces involved in dimer formation with chain *B* are clearly distinct in these two crystal structures.

structure of the MBP moieties is very similar in these two crystal structures, with r.m.s. deviations of corresponding MBP C^{α} positions ranging between 0.40 and 0.56 Å. However, the C-terminal peptides are different. In MalE-B363 the conformation of the C-terminal peptide is different in each of the three molecules of MalE-B363. In one molecule the peptide is completely ordered, in the second it is partially ordered and in the third it is entirely unstructured. In MBP-V_1(Ct) there is only electron density for the first five and six residues of the linker in the two molecules of the asymmetric unit, respectively.

MBP-fusion proteins can serve as an important tool to express and crystallize proteins that are otherwise intractable to structural investigation, but as this study shows the partner protein of interest may not be structured in the crystals of the fusion protein.

This work was funded by grant HL39757 from the National Institutes of Health to MS and MT. We thank the staff of the Structural Biology Center at the Advanced Photon Source, Argonne, Illinois for allocation of beam time at beamline BM19 as well as for expert assistance in data collection. Laura Mizoue from the Center for Structural Biology at Vanderbilt University is thanked for providing us with the modified pSV282 plasmid.

References

Berrada, K., Plesnicher, C., Luo, X. & Thibonnier, M. (2000). *J. Biol. Chem.* **275**, 27229–27237.
Brünger, A. T., Adams, P. D., Clore, G. M., DeLano, W. L., Gros, P., Grosse-Kunstleve, R. W., Jiang, J.-S., Kuszewski, J., Nilges, N., Pannu, N. S., Read, R. J., Rice, L. M., Simonson, T. & Warren, G. L. (1998). *Acta Cryst.* D**54**, 905–921.
Chao, J. A., Prasad, G. S., White, S. A., Stout, C. D. & Williamson, J. R. (2003). *J. Mol. Biol.* **326**, 999–1004.
Duan, X. & Quiocho, F. A. (2002). *Biochemistry*, **41**, 706–712.
Jones, T. A., Zou, J. Y., Cowan, S. W. & Kjeldgaard, M. (1991). *Acta Cryst.* A**47**, 110–119.
Laskowski, R. A., MacArthur, M. W., Moss, D. S. & Thornton, J. M. (1993). *J. Appl. Cryst.* **26**, 283–291.
Liu, Y., Manna, A., Li, R. G., Martin, W. E., Murphy, R. C., Cheung, A. L. & Zhang, G. Y. (2001). *Proc. Natl Acad. Sci. USA*, **98**, 6877–6882.
Otwinowski, Z. & Minor, W. (1997). *Methods Enzymol.* **276**, 307–326.
Palczewski, K., Kumasaka, T., Hori, T., Behnke, C. A., Motoshima, H., Fox, B. A., Le Trong, I., Teller, D. C., Okada, T., Stenkamp, R. E., Yamamoto, M. & Miyano, M. (2000). *Science*, **289**, 739–745.
Saul, F. A., Normand, B. V., Lema, F. & Bentley, G. A. (1998). *J. Mol. Biol.* **280**, 185–192.
Smyth, D. R., Mrozkiewicz, M. K., McGrath, W. J., Listwan, P. & Kobe, B. (2003). *Protein Sci.* **12**, 1313–1322.
Thibonnier, M., Coles, P., Thibonnier, A. & Shoham, M. (2001). *Annu. Rev. Pharmacol. Toxicol.* **41**, 175–202.
Thibonnier, M., Conarty, D. M., Preston, J. A., Wilkins, P. L., Berti-Mattera, L. N. & Mattera, R. (1998). *Adv. Exp. Med. Biol.* **449**, 251–276.
Thibonnier, M., Plesnicher, C., Berrada, K. & Berti-Mattera, L. (2001). *Am. J. Physiol.* **281**, E81–E92.
Wright, P. E. & Dyson, H. J. (1999). *J. Mol. Biol.* **293**, 321–331.